Geotechnical Aspects of Underground Construction in Soft Ground – Ng, Huang & Liu (eds)
© 2009 Taylor & Francis Group, London, ISBN 978-0-415-48475-6

Reinforcing effects of forepoling and facebolts in tunnelling

K. Date
Kajima Technical Research Institute, Kajima Corporation, Tokyo, Japan

R.J. Mair & K. Soga
Engineering Department, University of Cambridge, Cambridge, UK

ABSTRACT: Ground deformation induced by tunnelling in shallow sandy ground can be reduced by placing some reinforcements such as facebolts and forepoling bolts from the tunnel. A series of centrifuge tests have been carried out in order to investigate the ground deformation pattern during tunnel excavation with reinforcements. Three dimensional numerical analysis of the problem was also performed using FLAC3D and the simulation results show good agreement with the centrifuge data.

1 INTRODUCTION

Tunnel reinforcement has been applied to bored tunnel excavation in order to keep the cutting face stable, to reduce ground (sub)surface settlements and to avoid any adverse influence on adjacent structures. Forepoling and facebolts are the two most popular tunnel reinforcements; the former is often used in European countries, whereas the latter is frequently applied in Asian countries. However, the specifications of using them are based on local and empirical designs or on experience of past constructions in similar ground conditions.

In order to excavate a larger tunnel under poor ground conditions safely, it is necessary to establish a new design method for tunnel reinforcements such as forepoling and facebolts. In particular, in order to evaluate the relative merit of these two techniques for ground deformation control, it is important to compare them using the same modeling techniques (centrifuge tests or numerical analysis) under the same ground conditions.

2 CENTRIFUGE TESTS

In this study, the effect of tunnel reinforcements on ground deformation in shallow tunnels was investigated. Chambon and Corté (1994) performed centrifuge modeling of tunneling in sandy ground and showed the minimum pressure to support a cutting face was independent of cover diameter ratio (C/D, C: cover, D: tunnel diameter). They also showed, when a model tunnel was installed with C/D = 4 and P = 0.1D (P: unsupported length), the failure lines extended to the height of about 2.5D from the crown and did not extend to the ground surface. The centrifuge tests by Leca and Dormieux (1990) show that the failure lines reached the ground surface when C/D = 1. These two studies indicate that ground deformation pattern, when C/D is less than 1.0, is different from that C/D exceeds 1.0. Hence, it was decided to perform centrifuge experiments with a tunnel model of C/D = 1.0.

2.1 *Models*

A schematic view of the model is shown in Figure 1. The strong box shows the half of the prototype so that the ground deformation changes could be observed through a perspex window that is installed on the longitudinal section of the model. The ground deformation was analyzed using PIV program developed by White & Take (1996).

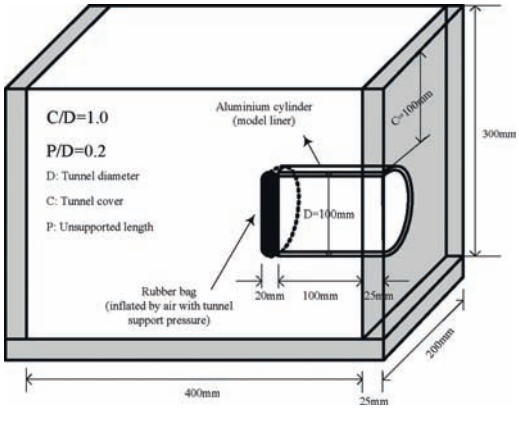

Figure 1. Schematic view of strong box and model tunnel.

Table 1. Matrix of reinforcement bolts.

Test	Type	Arrangement*	Number
KDC10	No reinforcement	–	0
KDC04	Facebolts	FB01	14
KDC05	Facebolts	FB02	14
KDC06	Forepoling	FP01	14
KDC07	Forepoling	FP02	28

* Each pattern is displayed in Figure 2.

The model box was filled with dry Leighton Buzzard Fraction E Silica sand with the relative density of 87% (±2%), corresponding to a unit weight of 15.9 kN/m^3.

The model tunnel, of diameter D = 100 mm (7.5 m in prototype), is semicircular and the depth to the tunnel crown C was equal to the diameter D (C/D = 1.0). The excavation of the tunnel was simulated by decreasing the internal pressure of a rubber bag placed at the tunnel face. The bag was covered with an alminium rigid lining, which was installed at a distance of P (=0.2D) behind the tunnel heading. The internal pressure was reduced from 100 kPa to tunnel collapse pressure. The centrifuge tests were performed at 75 g.

A series of five tests were carried out as listed in Table 1. The model reinforcement bolts, which were made of alminium, were installed perpendicularly to the tunnelling head during the sand-pouring. They were coated with the same sand as used in the tests, the outer diameter of them were 2.4 mm (180 mm in prototype). The forepoling model bolts were attached to the model liner with glue. The number, the length and the arrangement of the reinforcements were varied as shown in Table 1 and Figure 2.

2.2 *Tunnel collapse*

The model tunnel without tunnel reinforcement (KDC10) collapsed at the support pressure of 3.1 kPa, which agrees with the past centrifuge results by Chambon & Corté (1994). On the other hand, for the tunnels with reinforcements (KDC04-07), tunnels collapsed at lower pressures (2.2–2.7 kPa). This shows that not only facebolts but also forepoling contributes to reducing the minimum support pressure, but both techniques did not dramatically decrease the pressure required to keep the face stability.

The tunnel collapse mechanism on the longitudinal section is shown in Figure 3. When there is no reinforcement (KDC10), the front slippage line started at the bottom of the tunnel, extended upwards with a quasi-logarithmic curve, and then reached to the ground surface vertically. The line behind the tunnel was nearly vertical but a little inclined backwards. The failure mechanisms using facebolts are shown by KDC04 and 05 in Figure 3. The distinct difference from the non-reinforcement case was found at the front failure line, which started from some point at the upper face and then did not extend ahead of the face but extended upwards almost vertically. This showed that facebolts were effective to improve the face stability. In other words, this change in failure mechanism led to the reduction of the collapse volume. When facebolts were installed only at the upper face (KDC05), a chimney-like collapse was observed. This may be because the tunnel collapse was more dominated by P, that is, the stress relaxation at the crown rather than the height of the model tunnel, H.

When forepoling was introduced in a sparse manner (KDC06), the front slippage line was similar to that of non-reinforcement case (KDC10), but the back slippage line did not develop outward but inward toward the tunneling direction. This back line pattern was similar to that when a denser pattern of forepoling was introduced in KDC07. However, the geometry of the front line was totally different. In KDC07, the slippage line developed from the middle of the heading, and extended up to the horizontal line where forepoling bolts are embedded. Then the line suddenly developed vertically upwards to the ground surface.

When forepoling bolts are densely installed, they divide the surrounding ground into two zones; (a) the outside zone of invisible arch consisting of forepoling bolts, and (b) the inside zone of the forepoles. The mechanisms of collapse of the two zones have to be considered separately. It appears that the collapsed area shifted forward in the longitudinal direction.

2.3 *Changes in displacement vectors with the decrease in tunnel support pressure*

The ground deformation in sandy ground is quite small even when tunnel support pressure decreases to about half of the initial pressure. However, once it starts to develop, it abruptly increases and then reaches the collapse rather instantaneously. Therefore, in the past, it has been difficult to obtain the displacement vectors in sandy ground as the tunnel support pressure decreases. The PIV analysis, developed by White et al. (2003), was used to monitor subtle changes in ground deformation in sandy ground.

Figure 4 shows that the changes in the distribution of displacement vectors on the longitudinal section in KDC10 as the tunnel support pressure decreases. The displacement vectors were difficult to be detected even by using the PIV analysis until the internal stress was unloaded to around 25 kPa. Initially, the region deformed by the stress release was widespread. As shown in Figure 4, with decrease in the tunnel support pressure, the deformation became more localized around the face rubber bag. The first large ground movement was observed at 5.4 kPa and it was an ear-like shape on the longitudinal section. The observed

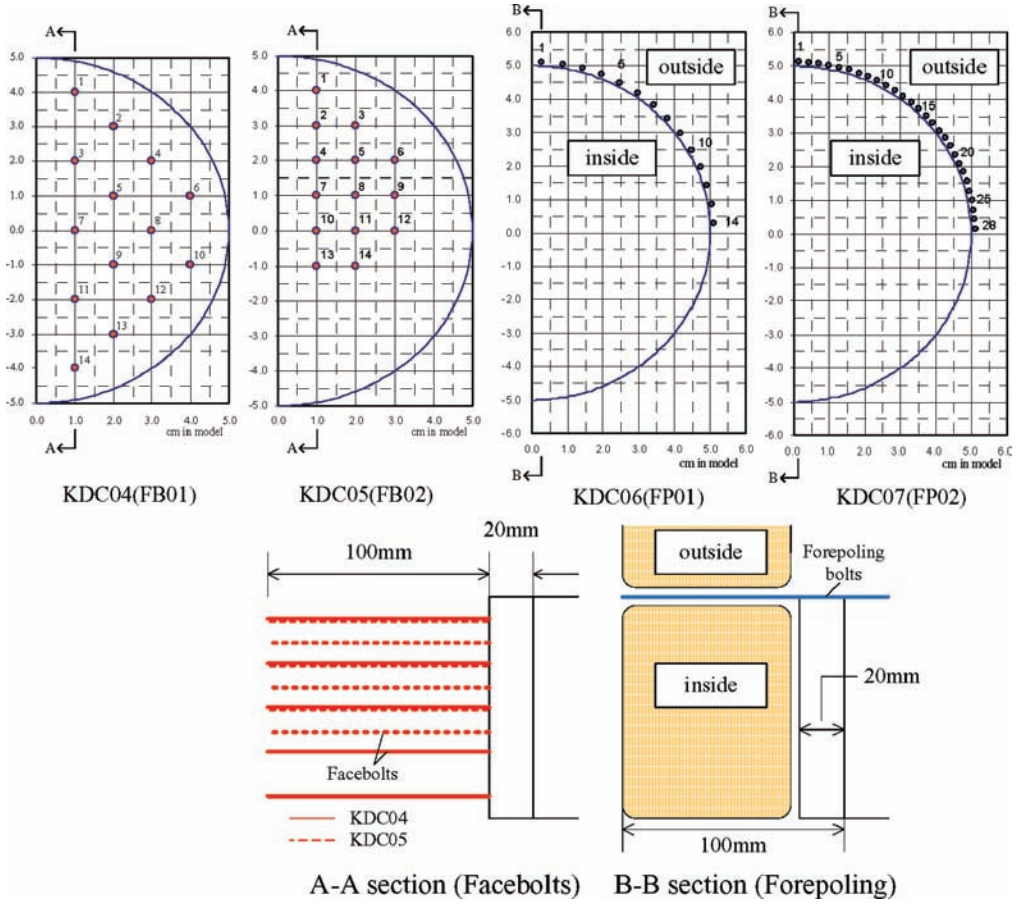

Figure 2. The arrangement patterns of bolts.

shape is similar to the three dimensional tunnel failure mechanism proposed by Leca & Dormieux (1990).

2.4 *Displacement vectors near collapse in centrifuge tests*

Figure 5 shows the displacement vectors at pressure close to the tunnel collapse, which varies from 3.5 to 5.0 kPa.

The distributions are comparable to the failure shapes shown in Figure 3. It was obvious from KDC04 and KDC05 that facebolts were effective to reduce the front area affected by tunnel excavation and also the ground movements, in particular, for the horizontal one. In the forepoling cases (KDC06 and KDC07), it appears that the ground moved under different mechanisms at the inside and outside of the half arches created by forepoling bolts as shown in Figure 1 and Figure 2. Some continuity between the inside and the outside is observed in KDC06, but they are discontinuous in KDC07. Hence, it was concluded that forepoling bolts can be effective to reduce the displacement outside the forepoling arch as long as they are installed densely enough to divide the surrounding ground into two zones.

Figure 6 shows the distribution of horizontal displacement along the cutting head at different internal pressures for KDC10, KDC04 and KDC07. Results show that facebolts (KDC04) contributed to the reduction of face extrusion. For the case of densely installed forepoling bolts (KDC07), the effect to reduce the face extrusion was not so apparent as that with facebolts, but the bulging pattern changed. That is, the maximum extrusion was found at the location beneath the crown, although it was found at about 1/4 the height of the face from the crown in KDC10 and KDC04. Ground deformation started at 20–25 kPa for all cases, but the deviation from the non-reinforcement case (KDC10) to the reinforcement cases (KDC04 and KDC07) became evident when the face pressure was 10–15 kPa.

In actual construction, great care must be taken in order to avoid fatal ground (sub)surface settlement above a tunnel, and hence it is essential to study how the settlement trough develops with the decrease in the tunnel pressure especially at locations just above the tunnel crown.

Figure 7 shows the subsurface settlement at just above the tunnel crown in KDC10, KDC04 and KDC07. These troughs appeared when the face pressure was 20–25 kPa for all cases, but the differences among them became apparent when the face pressure was 10–15 kPa. At around 5.5–6.5 kPa, the maximum settlements in KDC04 and KDC07 were about half as large as those in KDC10. Hence, both facebolts

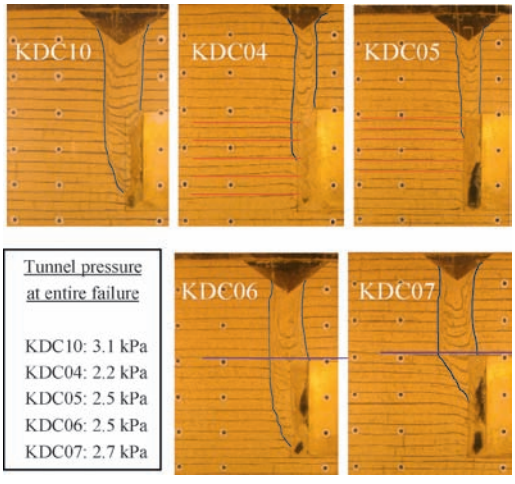

Figure 3. Tunnel failure patterns on the longitudinal section.

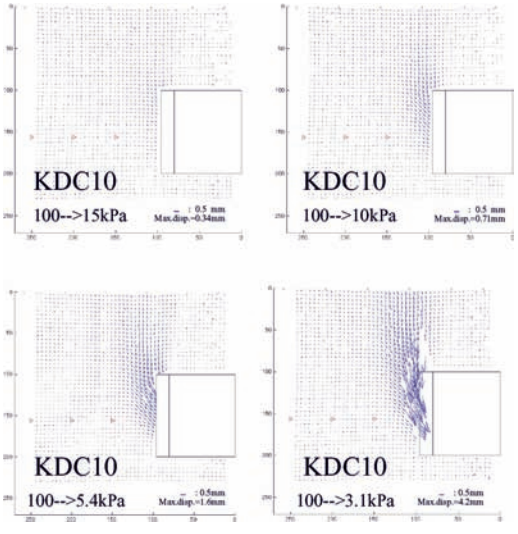

Figure 4. Displacement vector changes with the decrease in tunnel support pressure.

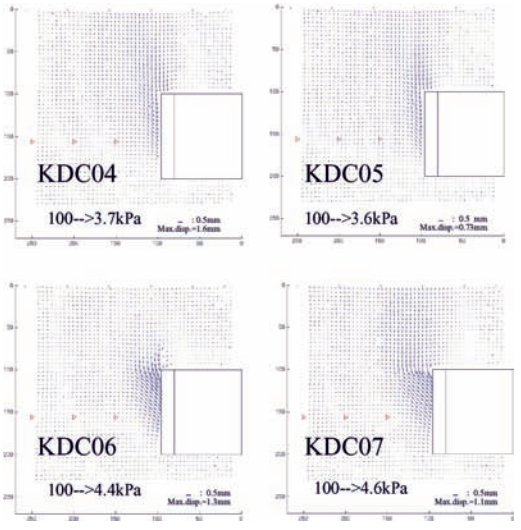

Figure 5. Displacement vector distribution on the longitudinal section.

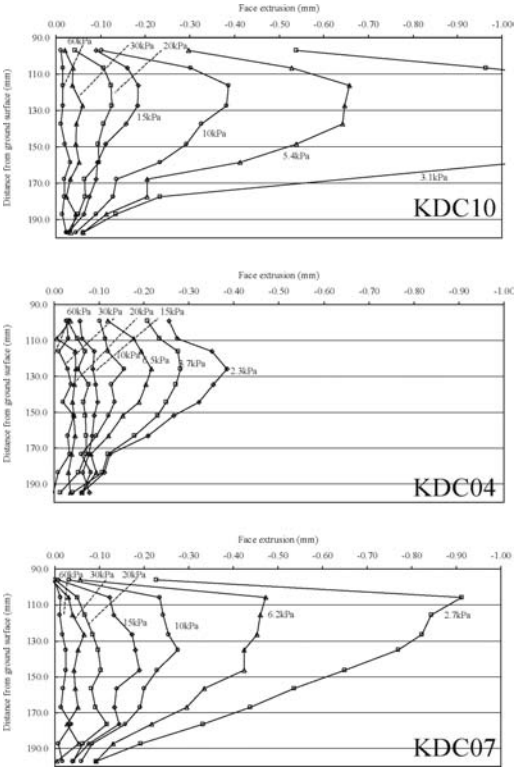

Figure 6. Distribution of face extrusion at the face.

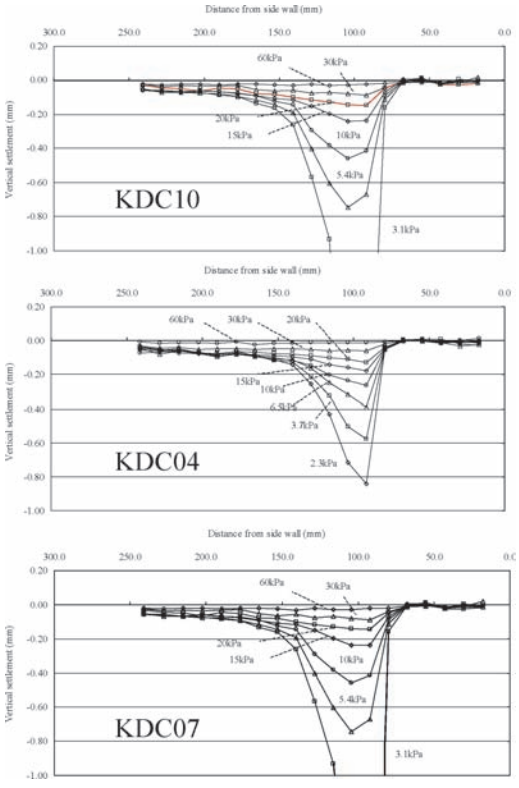

Figure 7. Subsurface settlement just above crown.

and forepoling were effective to reduce ground settlements. The shapes of the troughs are sharper in KDC10 and KDC04 than in KDC07. The maximum settlement in KDC4 was positioned behind that in KDC10. The trough in KDC07 was wider than the troughs observed in KDC04 and 10, and, as a result, the position of maximum settlement shifted ahead of the maximum settlement occurred in KDC10. Densely installed forepoling bolts were capable of reducing the influences from the stress release at both the face and the crown, while facebolts only contributed to counteract the effect of the stress release at the face.

3 SIMULATION MODELING AND ANALYSIS

3.1 *Modeling*

In order to simulate the centrifuge test results, 3D analyses were performed using FLAC3D. The geometry was identical to the internal size of the strong box used in the centrifuge modeling tests; 400 × 200 × 300 h in mm, as shown in Figure 8. For the boundary conditions at side walls, roller conditions were applied. The analysis basically followed the order of the centrifuge

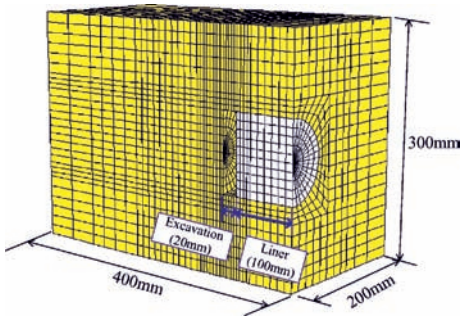

Figure 8. Geometry of 3D numerical analysis model.

Table 2. Soil properties for test simulation with FLAC3D.

Model	Young's modulus E	c(Pa)	$\phi(^\circ)$	$\psi(^\circ)$
Mohr-Coulomb-1*	$E = p' * 1400$ $p' = (\sigma_v + \sigma_h + \sigma_h)/3$	0.1	40	0, 15
Mohr-Coulomb-2**	$\sigma_h = \sigma_v * \nu/(1-\nu)$	0.1	See Figure 9	

* Mohr-Coulomb model 'without' strain softening/hardening model
** Mohr-Coulomb model 'with' strain softening/hardening model

tests; swing-up to 75 g, and then decrease of the internal pressure inside the rubber bag. The tunnel lining was assumed to be rigid.

3.2 *Soil property*

Mohr-Coulomb without strain softening/hardening model (MC), one of the standard and basic models, was used. Two dilation angles were used as shown in Table 2.

In addition, in order to simulate more accurately the results from the centrifuge tests, Mohr-Coulomb with strain softening/hardening model (SSH) was also used. The changes in parameters with plastic shear strain were derived from the triaxial tests by Coelho et al.(2007). As shown in Figure 9, the simulation of triaxial test results using FLAC3D showed good agreement with the test performed under the initial confining stress of 120 kPa.

3.3 *Simulation results for the non-reinforcement case*

Figure 10 shows the development of the maximum face extrusions with the decrease in the tunnel support pressure. The centrifuge exhibited the entire collapse at 3.1 kPa. The prediction with the SSH model was in good agreement with the experimental results. When the MC models were used, the deviation from the experimental results starts at around 30–40 kPa and

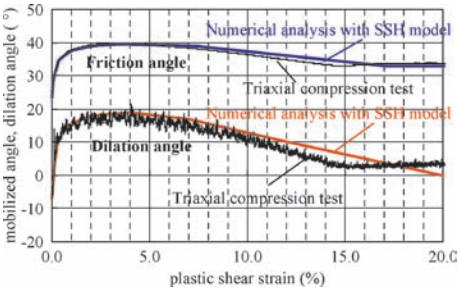

Figure 9. Simulation results of triaxial test at $\sigma_3 = 120$ kPa.

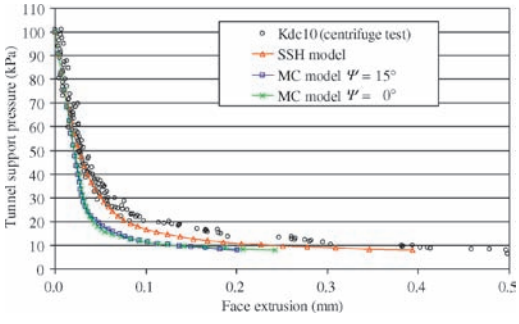

Figure 10. Simulation of the maximum face extrusion in KDC10 with 3D numerical analysis with the Mohr-Coulomb models with/without strain softening/hardening model.

then abrupt increase in face extrusion was found at around 15 kPa.

This is because the SSH model is able to simulate the plastic behaviour at and after small strain levels, corresponding to the face extrusion larger than 1.5 mm. As a result, the SSH model can follow the gradual increase in face extrusion with the decrease in tunnel support pressure.

Figure 11 shows the simulation results of the distribution of face extrusion in KDC10 when the tunnel support pressure was 8.0–9.0 kPa. Both constitutive models were successful in estimating the extrusion curve just before tunnel collapse, but, in order to simulate the deformation pattern observed in the experiments more precisely, the SSH model was found to be more appropriate than Mohr-Coulomb model.

However, there was a difference in position where the maximum extrusion occurred in Figure 11. In the numerical analyses, the peak was found at the middle and this location is lower than the location of the peak observed in the centrifuge test. This may be due to the difference in the shape of the excavation ranges in between centrifuge tests and numerical analyses. The model ground in centrifuge tests can move smoothly at the corner near the crown and the face because the rubber bag is flexible enough to be smoothly deformed. However, as for the numerical

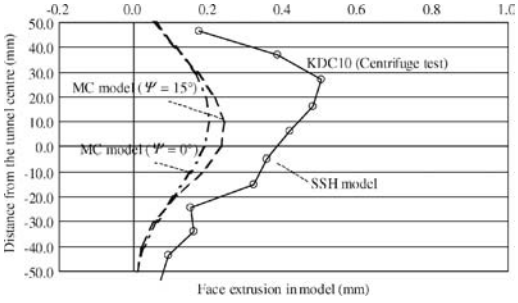

Figure 11. Simulation of the face extrusion bulges in KDC10 when the support pressure was 8.0–9.0 kPa.

Table 3. Input parameters for facebolts.

Model	Density	Young's modulus	Poisson's ratio
Pile	2700(kg/m^3)	7*10^4(MPa)	0.2

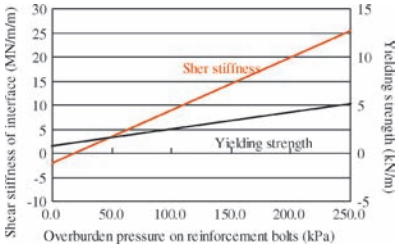

Figure 12. Changes in shear stiffness and yielding strength of soil-bolt interface with overburden pressure.

analyses, rectangular meshes might prevent the model ground from extruding inwards smoothly.

Further improvement in the numerical analysis (e.g. mesh making) is required in order to illustrate not only the development of the maximum extrusion but also its distribution along the face.

3.4 *Reinforcing effects of facebolts on reducing face extrusion*

The reduction of face extrusion by facebolts was also simulated. The SSH model was adopted for both simulations. The interface property between ground and bolt surface, which is shown in Table 3 and Figure 12, was derived from the pull-out tests reported in Date et al. (2007). Figure 13. shows the simulation results of KDC04. Results from KDC10 are also presented for comparison purpose.

The deformation pattern simulated by the numerical analysis was similar to that of the centrifuge test, but the magnitude predicted by the numerical analysis was

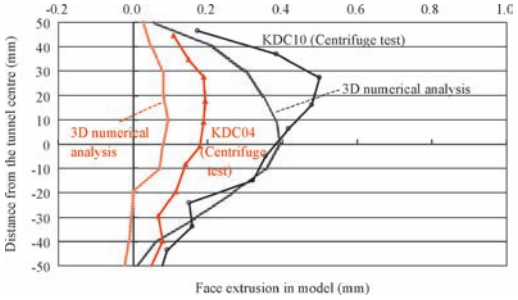

Figure 13. Simulation of face extrusion in KDC4 with 3D numerical analysis with the SSH model.

smaller than the centrifuge data. This may be due to the mesh problem mentioned above, the difference in the soil-bolt interaction properties and the difference in soil properties during between loading and excavating. Further investigation is needed.

4 CONCLUSIONS

A series of the centrifuge tests showed that introduction of facebolts and forepoling bolts for tunneling in shallow sandy ground yielded different shapes of tunnel collapse and contributed to some reduction in the tunnel support pressure to keep the cutting head stable. These techniques were also effective in reducing the vertical settlement at locations just above the tunnel crown. Facebolts were able to reduce the risk of face extrusion and hence can make the ground ahead of the face stiffer. Forepoling bolts can divide the ground around the tunnel face into two zones; the inside and the outside of the arch of forepoling bolts.

Numerical analysis results show that the SSH model (Mohr-Coulomb model with strain softening/hardening) gave better match to the centrifuge data than the MC model (Mohr-Coulomb model without strain softening/hardening). However, in order to simulate more realistic behaviour observed in the centrifuge tests, further investigation of the settings of numerical analysis such as mesh-making and soil-bolt interaction properties needs to be conducted.

REFERENCES

Chambon, P. & Corté, J.F. 1994. Shallow tunnels in cohesionless soil: stability of tunnel face. *Journal of Geotechnical and Geoenvironmental Engineering, ASCE, 120(7): 1150–1163 1994.*

Coelho, P.A.L.F. 2007. In situ densification as a liquefaction resistance measure for bridge foundations. *PhD Thesis, Cambridge University, UK., 2007.*

Date, K., Mair, R.J., Soga, K. Centrifuge tests for tunnel reinforcement. *Soils and Foundations, 2008.* (in preparation)

Leca, E., Dormieux, L. 1990. Upper and lower bound solutions for the face stability of shallow circular tunnels in frictional material. *Géotechnique 40(4), 581–606 1990.*

White, D., Take, A. Bolton, M.D. 2003. Soil deformation measurement using particle image velocimetry (PIV) and photogrammetry. *Géotechnique 53(7), 619–631 2003*.